
Exploring Adversarial Robustness of Deep Metric Learning

Thomas Kobber Panum¹ Zi Wang² Pengyu Kan² Earlence Fernandes² Somesh Jha²

Abstract

Deep Metric Learning (DML), a widely-used technique, involves learning a distance metric between pairs of samples. DML uses deep neural architectures to learn semantic embeddings of the input, where the distance between similar examples is small while dissimilar ones are far apart. Although the underlying neural networks produce good accuracy on naturally occurring samples, they are vulnerable to adversarially-perturbed samples that reduce performance. We take a first step towards training robust DML models and tackle the primary challenge of the metric losses being dependent on the samples in a mini-batch, unlike standard losses that only depend on the specific input-output pair. We analyze this dependence effect and contribute a robust optimization formulation. Using experiments on three commonly-used DML datasets, we demonstrate 5–76 fold increases in adversarial accuracy, and outperform an existing DML model that sought out to be robust.

1. Introduction

Many machine learning (ML) tasks rely on ranking entities based on the similarities of data points in the same class. Deep Metric Learning (DML) is a popular technique for such tasks, particularly for applications involving test-time inference of classes that are not present during training (e.g. zero-shot learning). Example applications of DML include person re-identification (Hermans et al., 2017), face verification (Schroff et al., 2015; Deng et al., 2019), phishing detection (Abdelnabi et al., 2020), and image retrieval (Wu et al., 2017; Roth et al., 2019). At its core, DML relies on state-of-the-art deep learning techniques for training models that output lower-dimensional semantic feature embeddings from high-dimensional inputs. Points in this embed-

ding space cluster similar inputs together while dissimilar inputs are far apart.

Traditional deep learning classifiers are vulnerable to adversarial examples (Szegedy et al., 2014; Biggio et al., 2013) — inconspicuous input changes that can cause the model to output attacker-desired values. Few studies have addressed whether DML models are similarly susceptible towards these attacks, and the results are contradictory (Abdelnabi et al., 2020; Panum et al., 2020). Given the wide usage of DML models in diverse ML tasks, including security-oriented ones, it is important to clarify their susceptibility towards attacks and ultimately address their lack of robustness. We investigate the vulnerability of DML towards these attacks and address the open problem of training DML models using robust optimization techniques (Ben-Tal et al., 2009; Madry et al., 2018).

A key challenge in robust training of DML models concerns the so-called *metric losses* (Wu et al., 2017; Wang et al., 2019; Chechik et al., 2010; Schroff et al., 2015). Unlike loss functions used in typical deep learning settings, the metric loss for a single data point is interdependent on other data points. For example, the widely-used triplet loss requires three input points: an anchor, a positive sample similar to the anchor, and a negative sample dissimilar to the anchor. For training, this interdependence impacts the effectiveness of learning (Wu et al., 2017). Thus, several works have identified sampling strategies that turn mini-batches into tuples or triplets to ensure that training remains effective (Schroff et al., 2015; Yuan et al., 2017; Xuan et al., 2020)

This *interdependence* between data points of metric losses poses a challenge for creating effective adversarial perturbations, as these are typically computed by approximating the inconspicuous noise that maximizes the loss for the specific data point. Consequently, as adversarial training depends on this ability during training, it has to remain efficient in order to reduce the additional computation as natural training procedures for certain DML models are already considered resource intensive (Roth et al., 2020). Additionally, metric losses are sensitive to samples with high levels of noise during training, that can cause training to reach an undesired local minima (Wu et al., 2017). Adversarial perturbations are effectively noise, and thus adversarial

¹Department of Electronic Systems, Aalborg University, Denmark ²Department of Computer Sciences, University of Wisconsin-Madison, Wisconsin, USA. Correspondence to: Thomas Kobber Panum <tkp@es.aau.dk>.

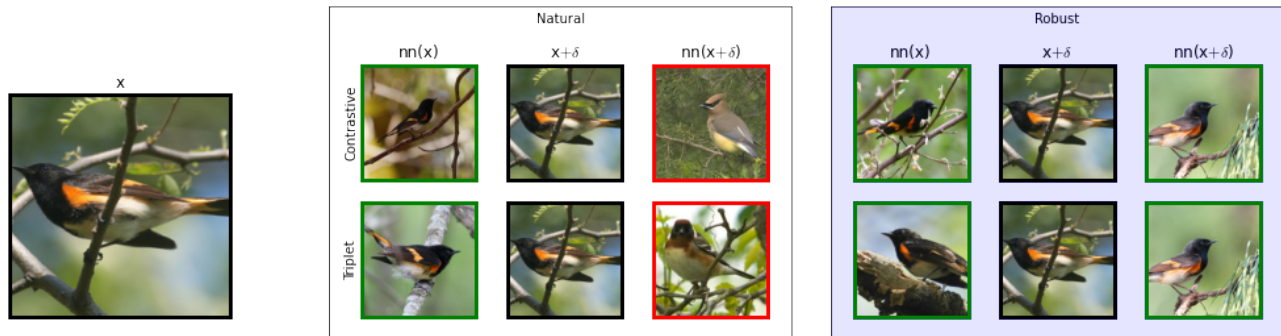


Figure 1. Example of inference of a naturally-trained DML model and robustly trained variant on the CUB200-2011 dataset. Each model infers the class of the natural data point x , and its perturbed $x + \delta$ counterpart, using the class of the nearest anchor $nn(\cdot)$. Green and red borders indicate correct- (same class) and incorrect inference, respectively. Both models infer the natural input correctly, however, the naturally-trained DML model fails to infer the adversarial perturbed input correctly.

training procedure for DML models has to account for this sensitivity.

We systematically approach the above challenges and contribute a robust training objective formulation for DML models by considering the two widely-used metric losses — contrastive and triplet loss. An example of the influence the robust training objective on inference is shown in Figure 1. Our key insight is that during an inference-time attack, adversaries seek to perturb data points such that the intra-class distance maximizes, and thus this behavior needs to be accounted for during training to improve robustness. Recent work has attempted to train robust DML models but has not considered the dependence and sensitivity to sampling (Abdelnabi et al., 2020). When we subject these models to our attack techniques, we find that their robustness is actually less than what is reported.

Prior work on traditional classifiers have established a connection between Lipschitz constant and robustness (Hein & Andriushchenko, 2017). Our intuition is the adversarial training of lead to a lower Lipschitz constant of the deep metric embedding. We explore this further in supplementary materials.

Contributions.

- We contribute a principled robust training framework for DML models by considering the dependence of metric losses on the other data points in the mini-batch and the sensitivity to sampling.
- We experiment with naturally-trained DML models across three commonly-used datasets for DML (CUB200-2011, CARS196, SOP) and show that they have poor robustness — their accuracy (R@1) drops from 59.1% (or more) to 4.0% (or less) when subjected to PGD attacks of the proposed attack formu-

lation.

- Using our formulation for adversarial training, DML models reliably increase their adversarial robustness, outperforming prior work. For $\ell_\infty(\epsilon = 0.01)$, we obtain an adversarial accuracy of 53.6% compared to the state-of-the-art natural accuracy baseline of 71.8% for the SOP dataset (in terms of R@1 score, a common metric in DML to assess the accuracy of models). Furthermore, the resulting robust model accuracies are largely unaffected for natural (unperturbed) samples.

2. Related Work

Deep Metric Learning. DML is a popular technique to obtain semantic feature embeddings with the property that similar inputs are geometrically close to each other in the embedding space while dissimilar inputs are far apart (Roth et al., 2020). DML losses involve pairwise distances between embeddings (Boudiaf et al., 2020). Examples include contrastive loss (Hadsell et al., 2006), triplet loss (Schroff et al., 2015), Neighborhood Component Analysis (Goldberger et al., 2004), and various extensions of these losses (Sohn, 2016; Wang et al., 2019; Zheng et al., 2019). Throughout this work, we refer to these types of losses as *metric losses*. Recent surveys (Roth et al., 2020; Musgrave et al., 2020) highlight that performance of newer metric losses are lesser than previously reported. Thus, we focus on the two established metric losses — contrastive and triplet — as they are widely used and have good performance.

Adversarial Robustness. Since early work in the ML community discovered adversarial examples in deep learning models (Szegedy et al., 2014; Biggio et al., 2013), a big focus has been to train adversarially-robust models. We

focus on robust optimization-based training that utilizes a saddle-point formulation (min-max) (Ben-Tal et al., 2009; Madry et al., 2018). To the best of our knowledge, training DML models using robust-optimization techniques has not been thoroughly studied, and only recently has work begun in this area (Abdelnabi et al., 2020).

Using the Generative Adversarial Network architecture (Goodfellow et al., 2014), Duan et al. (2018) create a framework that uses generative models during training to derive hard negative samples from easy negatives. They focus on improving the effectiveness of *naturally* training DML models rather than obtaining adversarial robustness, which is our focus.

Recent studies have shown that metric losses can function as a supplementary regularization method that enhances adversarial robustness of deep neural network classifiers (e.g., CNNs) (Mao et al., 2019; Li et al., 2019). However, these studies are not applicable to training robust DML models, as they do not solve the problem of dependence between data points due to the use of metric losses. We propose a principled framework for robustly training DML models that accounts for this problem.

3. Towards Robust Deep Metric Models

First, we describe some basic machine learning (ML) notation and concepts required to describe our algorithm. We assume a data distribution \mathcal{D} over $\mathcal{X} \times \mathcal{Y}$, where \mathcal{X} is the sample space and $\mathcal{Y} = \{y_1, \dots, y_L\}$ is the finite space of labels. Let $\mathcal{D}_{\mathcal{X}}$ be the marginal distribution over \mathcal{X} induced by \mathcal{D} ¹. Given $Y \subseteq \mathcal{Y}$ we define \mathcal{D}_Y to be the measure of the subsets of $\mathcal{X} \times Y$ induced by \mathcal{D} . For $y \in \mathcal{D}$, \mathcal{D}_y and \mathcal{D}_{-y} denote the measures $\mathcal{D}_{\{y\}}$ and $\mathcal{D}_{\mathcal{Y} \setminus \{y\}}$, respectively.

In the *empirical risk minimization (ERM)* framework we wish to solve the following optimization problem:

$$\min_{w \in \mathcal{H}} E_{(\mathbf{x}, y) \sim \mathcal{D}} l(w, \mathbf{x}, y) \quad (1)$$

In the equation given above \mathcal{H} is the hypothesis space and l is the loss function. We will denote vectors in boldface (e.g. \mathbf{x} , \mathbf{y}). Since the distribution is usually unknown, a learner solves the following problem over a data set $S = \{(\mathbf{x}_1, y_1), \dots, (\mathbf{x}_n, y_n)\}$ sampled from the distribution \mathcal{D} .

$$\min_{w \in \mathcal{H}} \frac{1}{n} \sum_{i=1}^n l(w, \mathbf{x}_i, y_i) \quad (2)$$

Once we have solved the optimization problem given above, we obtain a $w^* \in \mathcal{H}$ which yields a classifier $F: \mathcal{X} \rightarrow \mathcal{Y}$ (the classifier is usually parameterized by w^* , but we will omit it for brevity).

¹The measure of set $Z \subseteq \mathcal{X}$ in distribution $\mathcal{D}_{\mathcal{X}}$ is the measure of the set $Z \times \mathcal{Y}$ in distribution \mathcal{D} .

3.1. Deep Metric Models

The goal of *deep metric learning (DML)* is to create a *deep metric model* f_{θ} is function from \mathcal{X} to S^d , where $\theta \in \Theta$ is a parameter and S^d is an unit sphere in \mathbb{R}^d (i.e. $\mathbf{x} \in S^d$ iff $\|\mathbf{x}\|_2 = 1$). Since deep metric models embed a space \mathcal{X} (which can itself be a metric space) in another metric space, we also sometimes refer to them deep embedding. Frequently, deep metric models use very different loss functions than typical classification networks described previously. Next we discuss two kinds of loss functions – contrastive and triplet. Let $S = \{(\mathbf{x}_1, y_1), \dots, (\mathbf{x}_n, y_n)\}$ be a dataset drawn from \mathcal{D} . A *contrastive* loss function $l_c(\theta, (\mathbf{x}, y), (\mathbf{x}_1, y_1))$ of labeled samples from $\mathcal{X} \times \mathcal{Y}$ and is defined as:

$$1_{y=y_1} d_{\theta}(\mathbf{x}, \mathbf{x}_1) + 1_{y \neq y_1} [\alpha - d_{\theta}(\mathbf{x}, \mathbf{x}_1)] \quad (3)$$

In the equation given above, 1_E is an indicator function for event E (1 if event E is true and 0 otherwise), and $d_{\theta}(\mathbf{x}, \mathbf{x}_1)$ is $\sqrt{\sum_{j=1}^d (f_{\theta}(\mathbf{x})_j - f_{\theta}(\mathbf{x}_1)_j)^2}$, the ℓ_2 distance in the embedding space. The goal of the contrastive loss function is to reduce the distance in the embedding space between two samples with the same label, and analogously increase the distance in the embedding space between the two samples with different labels. A *triplet* loss function l_t is defined over three $l_t(\theta, (\mathbf{x}, y), (\mathbf{x}_1, y_1), (\mathbf{x}_2, y_2))$ labeled samples and is defined as follows:

$$1_{y=y_1} 1_{y \neq y_2} [d_{\theta}(\mathbf{x}, \mathbf{x}_1) - d_{\theta}(\mathbf{x}, \mathbf{x}_2) + \alpha]_+ \quad (4)$$

In the equation given above $[x]_+$ is $\max(x, 0)$. In order for the expression to be non-zero (\mathbf{x}_1, y_1) has to have the same label as (\mathbf{x}, y) , and (\mathbf{x}_2, y_2) has to have a different label as (\mathbf{x}, y) .

3.2. Attacks on Deep Metric Models

Assume that we have learned a deep embedding network with parameter $\theta \in \Theta$ using one of the loss functions described above. Next we describe how the network is used. Let $A = \{(\mathbf{a}_1, c_1), \dots, (\mathbf{a}_m, c_m)\}$ be a reference or test dataset (e.g. a set of faces along with their label). A is distinct from the dataset S used during training time. Suppose we have a sample \mathbf{z} and let $k(A, \mathbf{z})$ be the index that corresponds to $\arg \min_{j \in \{1, \dots, m\}} d_{\theta}(\mathbf{a}_j, \mathbf{z})^2$. We predict the label of \mathbf{z} as $lb(A, \mathbf{z}) = c_{k(A, \mathbf{z})}$ (we will use the functions $k(\cdot, \cdot)$ and $lb(\cdot, \cdot)$ throughout this section).

Next we describe test-time attacks on a deep embedding with parameter θ . Let $\mathbf{z} \in \mathcal{X}$. *Untargeted attack* on \mathbf{z} can be described as follows (we want the perturbed point

²In case one or more anchors share the minimal distance to \mathbf{z} , the tie is broke by a random selection among these anchors.

to have a different label than before):

$$\min_{\delta \in \mathcal{X}} \mu(\delta) \quad \text{such that } lb(A, \mathbf{z}) \neq lb(A, \mathbf{z} + \delta) \quad (5)$$

Targeted attack (with a target label $t \neq lb(A, \mathbf{z})$) can be described as follows (we desire to the predicted label of the perturbed point to be a specific label):

$$\min_{\delta \in \mathcal{X}} \mu(\delta) \quad \text{such that } lb(A, \mathbf{z} + \delta) = t \quad (6)$$

In the formulations given above we assume that \mathcal{X} is a metric space with μ a metric on \mathcal{X} (e.g. \mathcal{X} could \mathbb{R}^n with usual norms, such as ℓ_∞ , ℓ_1 , or ℓ_p (for $p \geq 2$)). Any algorithm that solves the optimization problem described above leads to a specific attack on deep metric models.

3.3. Robust Deep Metric Models

Let $S = \{(\mathbf{x}_1, y_1), \dots, (\mathbf{x}_n, y_n)\}$ be a dataset drawn from distribution \mathcal{D} . For a sample (\mathbf{x}_i, y_i) where $1 \leq i \leq n$ we define the following surrogate loss function $\hat{l}(\theta, (x_i, y_i), S)$ for the contrastive loss function l_c :

$$\hat{l}(\theta, (x_i, y_i), S) = \frac{1}{n} \sum_{j=1}^n l_c(\theta, (\mathbf{x}_i, y_i), (\mathbf{x}_j, y_j)) \quad (7)$$

Similarly, for the triplet loss function l_t we can define the following surrogate loss function $\hat{l}(\theta, (x_i, y_i), S)$:

$$\frac{1}{n_{y_i} n_{\bar{y}_i}} \sum_{j=1}^{n_{y_i}} \sum_{k=1}^{n_{\bar{y}_i}} l_t(\theta, (\mathbf{x}_i, y_i), (\mathbf{x}_j, y_j), (\mathbf{x}_k, y_k)) \quad (8)$$

Let S_y and S_{-y} be defined as the following sets: $\{(\mathbf{x}, y) \mid (\mathbf{x}, y) \in S\}$ and $\{(\mathbf{x}, y') \mid (\mathbf{x}, y') \in S \text{ and } y' \neq y\}$. In the equation given above the sizes of the sets S_y and S_{-y} are denoted by n_y and $n_{\bar{y}}$, respectively.

Having defined the surrogate loss function \hat{l} the learner's problem can be defined as:

$$\min_{\theta \in \Theta} \frac{1}{n} \sum_{i=1}^n \hat{l}(\theta, (\mathbf{x}_i, y_i), S) \quad (9)$$

Recall that the learner's problem for the usual classification case is:

$$\min_{w \in \mathcal{H}} \frac{1}{n} \sum_{i=1}^n l(w, \mathbf{x}_i, y_i) \quad (10)$$

Note that in the classification case the loss function $l(w, \mathbf{x}_i, y_i)$ of a sample (\mathbf{x}_i, y_i) does not depend on the other samples in the dataset S . However, in the deep metric

model case the surrogate loss function $\hat{l}(\theta, (\mathbf{x}_i, y_i), S)$ for a sample (\mathbf{x}_i, y_i) depends on the rest of the data set S (see the equations for \hat{l}) This is the main difference between the embedding and classification scenarios.

Formulation 1. Let $B_p(\mathbf{x}, \epsilon)$ denote the ϵ -ball around the sample \mathbf{x} using the ℓ_p -norm. The straightforward robust formulation is given in the equation below.

$$\min_{\theta \in \Theta} \max_{(\mathbf{z}_1, \dots, \mathbf{z}_n) \in \prod_{j=1}^n B_p(\mathbf{x}_j, \epsilon)} \frac{1}{n} \sum_{i=1}^n \hat{l}(\theta, (\mathbf{z}_i, y_i), S) \quad (11)$$

In the formulation given above, all samples are adversarially perturbed at the same time (note that the max is outside the summation). Therefore, this formulation is not convenient for current training algorithms, such as SGD and ADAM. This is because the entire dataset S has to be perturbed at the same time. Moreover, this formulation is not conducive to various sampling strategies used in training of deep metric models.

Formulation 2. In this formulation we push the max inside the sum so that each term can be individually processed. This is especially useful for adversarial training because each tuple or triple can be perturbed separately. Our formulation will be indexed by r ($r \in \{1, 2\}$ for contrastive loss and $r \in \{1, 2, 3\}$ for triplet loss). Intuitively, r denotes what component of the tuple or triple is being perturbed. We define operator $\max(r, \epsilon, \theta)$ which perturbs the r -th component in an ϵ ball to maximize the loss. For example, $\max(r, \epsilon, \theta)$ for $((\mathbf{x}, y), (\mathbf{x}_1, y_1))$ is defined as:

$$\max_{\mathbf{z} \in B_p(\mathbf{x}_1, \epsilon)} l_c(\theta, (\mathbf{x}, y), (\mathbf{z}, y_1)) \quad (12)$$

Now we can define \hat{l}_r for the contrastive case as:

$$\hat{l}_r(\theta, (x_i, y_i), S) = \frac{1}{n} \sum_{j=1}^n \max(r, \epsilon, \theta)((\mathbf{x}_i, y_i), (\mathbf{x}_j, y_j))$$

The equation for the triplet loss is similar. Now the entire minimization problem becomes.

$$\min_{\theta \in \Theta} \frac{1}{n} \sum_{i=1}^n \hat{l}_r(\theta, (\mathbf{z}_i, y_i), S) \quad (13)$$

Formulation 3. Our third formulation adds a regularizer which enforces the following informal constraint: if \mathbf{x} changes a bit, the distance in the embedding space does not change too much.

$$\min_{\theta \in \Theta} \frac{1}{n} \sum_{i=1}^n [\hat{l}(\theta, (\mathbf{x}_i, y_i), S) + \lambda \max_{\mathbf{z} \in B_p(\mathbf{x}_i, \epsilon)} d_\theta(\mathbf{z}, \mathbf{x}_i)] \quad (14)$$

These robust optimization formulations follow the common notion of robustness from robust optimization (Ben-Tal et al., 2009), thus given an algorithm for solving one

of the robust optimization formulations, leads to a robust model.

3.4. Attack Algorithm

We will focus on untargeted attacks because our main goal is to use these algorithms to robustify embeddings using adversarial training. Recall that $d_\theta(\mathbf{x}, \mathbf{x}_1)$ is the l_2 distance between $f_\theta(\mathbf{x})$ and $f_\theta(\mathbf{x}_1)$. The gradient $\nabla_{\mathbf{x}} d_\theta(\mathbf{x}, \mathbf{x}_1)$ of $d_\theta(\mathbf{x}, \mathbf{x}_1)$ with-respect-to (wrt) to \mathbf{x} is given by:

$$\frac{1}{d_\theta(\mathbf{x}, \mathbf{x}_1)} (f_\theta(\mathbf{x}) - f_\theta(\mathbf{x}_1))^T \cdot \nabla_{\mathbf{x}} f_\theta(\mathbf{x}) \quad (15)$$

A similar expression can be written for $\nabla_{\mathbf{x}_1} d_\theta(\mathbf{x}, \mathbf{x}_1)$.

Consider the contrastive loss l_c on a tuple $(\mathbf{x}, \mathbf{x}_1)$.

$$1_{y=y_1} d_\theta(\mathbf{x}, \mathbf{x}_1) + 1_{y \neq y_1} [\alpha - d_\theta(\mathbf{x}, \mathbf{x}_1)] \quad (16)$$

The gradient of the contrastive loss $\nabla_{\mathbf{x}_1} l_c(\theta, (\mathbf{x}, y), (\mathbf{x}_1, y_1))$ wrt \mathbf{x}_1 is shown below:

$$1_{y=y_1} \nabla_{\mathbf{x}_1} d_\theta(\mathbf{x}, \mathbf{x}_1) - 1_{y \neq y_1} \nabla_{\mathbf{x}_1} d_\theta(\mathbf{x}, \mathbf{x}_1) \quad (17)$$

Similar to contrastive loss, we can define gradients of $l_t(\theta, (\mathbf{x}, y), (\mathbf{x}_1, y_1), (\mathbf{x}_2, y_2))$ wrt \mathbf{x} , \mathbf{x}_1 , or \mathbf{x}_2 .

Once we can compute the gradients of the loss, we can readily adapt attack algorithm, such as FGSM and PGD, to our context. Note that for formulation 3 we need to only compute the gradient of In fact any attack algorithm that only relies on gradients of the loss function can be adapted for our case. For example the PGD attack can be adapted for contrastive loss l_c as follows:

$$\mathbf{x}_1^{t+1} = \Pi_{\mathbf{x}_1 + B_p(\epsilon)}(\mathbf{x}_1^t + \alpha \nabla_{\mathbf{x}_1} l_c(\theta, (\mathbf{x}, y), (\mathbf{x}_1, y_1)))$$

In the equation we are showing one iteration of the PGD and $B_p(\epsilon)$ is the ϵ ball centered at the origin using the l_p norm. For computational reasons, in our attack algorithms we only perturb one of the components for the tuples of triples.

3.5. Adversarial Training

Once we have the attack algorithm, adversarial training for robustifying the model is relatively straightforward. We assume that the attack algorithm only perturbs one component of the tuple or triple. Let $\mathcal{A}_r^c(\cdot, \cdot)$ ($r \in \{1, 2\}$) and $\mathcal{A}_r^t(\cdot, \cdot, \cdot)$ ($r \in \{1, 2, 3\}$) be the attack algorithms for the contrastive and the triple losses, respectively. In the attack

algorithms given above r refers to the index of the component being perturbed (e.g. $\mathcal{A}_2((\mathbf{x}, y), (\mathbf{x}_1, y_1))$ and returns $((\mathbf{x}, y), (\mathbf{x}_1 + \delta, y_1))$. Next we describe adversarial training for contrastive loss (the case for triple loss is similar). $\mathcal{A}(\mathbf{x})$ corresponds to formulation 3 (attempts to solve $\max_{\mathbf{z} \in B_p(\mathbf{x}, \epsilon)} d_\theta(\mathbf{z}, \mathbf{x})$).

As pointed before, formulation 1 is computationally prohibitive. We will focus on formulations 2 and 3. Let $S = \{(\mathbf{x}_1, y_1), \dots, (\mathbf{x}_n, y_n)\}$ be the dataset. At each iteration, a tuple $T = ((\mathbf{x}_i, y_i), (\mathbf{x}_j, y_j))$ is sampled from S . We construct the tuple T' from T using attack algorithm (i.e. $T' = \mathcal{A}_r^c(T)$ or $T' = \mathcal{A}_r^t(T)$), and run one step of the learning algorithm, such as SGD or ADAM, on T' . This corresponds to formulation 2. For formulation 3 we use attack algorithm \mathcal{A} .

4. Experiments

Our experiments explore the following research questions:

Q1. How robust are *naturally* trained DML models towards established adversarial example attacks?

Among commonly used datasets for visual similarity, we find that DML models, trained with state-of-the-art parameter choices, are vulnerable to adversarial examples, similar to non-DML models (Table 1). This forms our baseline for adversarial robustness.

Q2. What is the accuracy of DML models when they are trained using our robust formulation?

We find that DML models can be trained to become more robust across a variety of norms. For example, for a PGD attack with 5 iterations under l_∞ ($\epsilon = 0.01$), we increase the adversarial accuracy to 53.6% compared from the state-of-the-art natural baseline of 0.2% for contrastive loss on the SOP dataset (Table 1).

Q3. How does the robust training objective affect the learned embedding space?

Using a synthetic dataset, we demonstrate that the proposed adversarial training reduces the amount of shifting that adversarial perturbations can cause in the embedding space (Figure 2).

We run all experiments on Nvidia Tesla V100 GPUs (32 GB) RAM. Our code is available at (anonymized repository) <https://github.com/anonymous-koala-supporter/adversarial-deep-metric-learning>.

Table 1. Performance of DML models across datasets, types of perturbations, and attack algorithms. Results are an average of five random seeds and best performances for a given combination of input data (*Benign*, $\ell_2(\epsilon = 4)$, $\ell_\infty(\epsilon = 0.01)$) and dataset is marked in **bold**. We highlight our robust training technique using a shaded background and suffix them by their trained norm (e.g. (ℓ_∞)). Recall that, R@1 reflects a model’s inference accuracy, while mAP@R reflects its ability to rank similar entities. Naturally-trained DML models (Contrastive, Triplet) demonstrate low robustness towards the proposed attack formulation across the adversarial settings ($\ell_2(\epsilon = 4)$, $\ell_\infty(\epsilon = 0.01)$). Our robust training objective improves robustness towards adversarial attacks, and outperforms previous attempts at establishing robust DML models (VisualPhishNet).

Model	Attack	CUB200-2011		CARS196		SOP		VisualPhish	
		R@1	mAP@R	R@1	mAP@R	R@1	mAP@R	R@1	mAP@R
<i>Benign (Natural samples)</i>									
Contrastive	—	59.1 ± 0.0	21.0 ± 0.0	74.0 ± 0.0	20.9 ± 0.0	71.8 ± 0.0	44.7 ± 0.0	78.2 ± 0.0	73.6 ± 0.0
Triplet	—	59.3 ± 0.0	21.7 ± 0.0	74.0 ± 0.0	21.4 ± 0.0	69.6 ± 0.0	42.1 ± 0.0	81.9 ± 0.0	77.0 ± 0.0
VisualPhishNet	—	N/A						64.0 ± 0.0	17.6 ± 0.0
Contrastive (ℓ_2)	—	55.6 ± 0.0	19.5 ± 0.0	71.6 ± 0.0	18.8 ± 0.0	66.3 ± 0.0	38.4 ± 0.0	76.0 ± 0.0	70.9 ± 0.0
Triplet (ℓ_2)	—	55.9 ± 0.0	19.8 ± 0.0	71.6 ± 0.0	18.8 ± 0.0	62.2 ± 0.0	34.6 ± 0.0	76.8 ± 0.0	73.8 ± 0.0
Contrastive (ℓ_∞)	—	58.2 ± 0.0	20.2 ± 0.0	72.1 ± 0.0	19.5 ± 0.0	66.7 ± 0.0	39.0 ± 0.0	76.8 ± 0.0	72.1 ± 0.0
Triplet (ℓ_∞)	—	53.4 ± 0.0	17.9 ± 0.0	71.9 ± 0.0	19.8 ± 0.0	64.0 ± 0.0	36.4 ± 0.0	79.1 ± 0.0	76.0 ± 0.0
$\ell_2(\epsilon = 4)$									
Contrastive	PGD	8.6 ± 0.2	4.8 ± 0.1	3.7 ± 0.2	2.4 ± 0.0	2.3 ± 0.0	2.3 ± 0.0	45.5 ± 0.2	43.1 ± 0.1
Triplet	PGD	9.6 ± 0.3	5.5 ± 0.1	2.9 ± 0.1	2.2 ± 0.0	1.2 ± 0.0	1.8 ± 0.0	34.6 ± 0.6	28.5 ± 0.1
Contrastive (ℓ_2)	PGD	26.4 ± 0.3	11.1 ± 0.0	37.2 ± 0.2	9.7 ± 0.0	51.6 ± 0.0	29.2 ± 0.0	56.6 ± 0.4	54.0 ± 0.2
Triplet (ℓ_2)	PGD	27.2 ± 0.2	11.3 ± 0.1	37.0 ± 0.4	9.3 ± 0.0	37.7 ± 0.1	20.3 ± 0.0	55.1 ± 0.1	50.9 ± 0.2
$\ell_\infty(\epsilon = 0.01)$									
Contrastive	PGD	3.9 ± 0.3	3.4 ± 0.1	1.4 ± 0.2	1.9 ± 0.0	0.7 ± 0.0	1.5 ± 0.0	35.7 ± 0.2	34.3 ± 0.2
Triplet	PGD	4.0 ± 0.3	3.8 ± 0.1	0.7 ± 0.0	1.7 ± 0.0	0.2 ± 0.0	1.3 ± 0.0	20.8 ± 0.1	16.8 ± 0.3
VisualPhishNet	PGD	N/A						42.8 ± 0.2	13.2 ± 0.0
Contrastive (ℓ_∞)	PGD	20.3 ± 0.5	8.8 ± 0.0	35.7 ± 0.2	9.7 ± 0.1	53.6 ± 0.0	30.4 ± 0.0	56.7 ± 0.2	53.6 ± 0.1
Triplet (ℓ_∞)	PGD	16.9 ± 0.1	7.4 ± 0.1	36.2 ± 0.5	9.6 ± 0.1	39.3 ± 0.1	21.3 ± 0.0	54.7 ± 0.1	49.1 ± 0.1

4.1. Experimental Setup

Datasets. We use the following four real-world image datasets for our experiments:

- **CUB200-2011** (Welinder et al., 2010): Images of birds across 200 species and have a total of 11 788 images.
- **CARS196** (Krause et al., 2013): Dataset with images of cars spanning across 196 models, with a total of 16 185 images.
- **SOP** (Song et al., 2016): Product images from eBay listings 120 053 images of 22 634 different online products.
- **VisualPhish** (Abdelnabi et al., 2020): Screenshots of benign websites, from a set of established brands, and phishing websites that attempt to replicate the visual appearance of their benign counterpart. It covers 146 brands across a total of 10 558 screenshots.

CUB200-2011, CARS196, and SOP are commonly used within the DML literature (Musgrave et al., 2020). These three datasets are divided into a training and testing set

of approximately the same size by selecting the first half of classes for the training set, while having the remaining classes be in the testing set (Roth et al., 2020). This setup reflects an out-of-distribution scenario — a common application of DML. VisualPhish is a newer dataset that underlies the robust phishing detection model, VisualPhishNet (Abdelnabi et al., 2020). For a fair comparison, we adopt the train-test split from the VisualPhish implementation. This yields a test set of 717 website screenshots. In addition to these real-world datasets, we also include the following synthetic dataset:

Synth Dataset: A dataset with two classes a and b where data points $\mathbf{x} \in [0, 1]^k$ and $k = 224 \times 224 \times 3$ to maintain identical dimensionality of the real-world datasets. Data points from each class are drawn from $\mathcal{N}(\mu, \sigma^2 I)$ st. $\sigma = 0.075$ while $\mu = 0.25$ for class a and $\mu = 0.75$ for class b .

Models & Training Parameters. We use default parameter choices from prior work that yield state-of-the-art performance on natural samples (Roth et al., 2020). Main parameters are summarized in this section and provide a complete listing in Appendix A. Deviations from the default parameter choices are discussed and emphasized.

All models are ResNet50 (He et al., 2016) initialized with pre-trained weights from an ImageNet classifier. We replace the last fully connected layer with another that matches the embedding space dimensionality. Embeddings are normalized to be on the n -dimensional unit sphere, where $n = 128$ throughout our experiments. We use ADAM (Kingma & Ba, 2015) with learning rate³ of 10^{-6} , weight decay of $4 \cdot 10^{-4}$. We use contrastive and triplet losses during training, setting $\alpha = 1.0$ and $\alpha = 0.2$, respectively.

To the best of our knowledge, VisualPhishNet is the only previous attempt at creating an adversarially robust DML model trained using metric losses. At the core, the model is a variant of the VGG16 (Simonyan & Zisserman, 2015) architecture with an unnormalized embedding layer of size 512. It was trained using the VisualPhish dataset and is expected to learn a visual similarity metric between web sites of various origins.

Training on the real-world datasets is performed over 150 epochs, with the exception of SOP that is trained for 100 epochs due to its volume (Roth et al., 2020). Mini-batches are of size 112 and sampled using the sampling technique SPC-2, which ensures that each batch contains exactly two samples per class for the selected classes in the batch.

Adversarial Robustness. To establish a benchmark for adversarial robustness, we employ the attack algorithm covered in Section 3.4. For each data point being perturbed, we sample the nearest positive neighbor to reflect the ideal attack setting for an adversary. The formulation uses Projected Gradient Decent (PGD) (Madry et al., 2018) because it is considered one of the strongest white-box attacks available (Wong et al., 2020). Each attack is run for five iterations ($i = 5$) and has a step size given by $2\epsilon\frac{1}{i}$, such that the step size remains small while not hindering the optimization from reaching any point within the ϵ -ball despite random initialization. Throughout the experiments we use the notation of $\ell_p(\epsilon = 0.01)$ to indicate that for any data point \mathbf{x} , its valid perturbations are contained in $B_p(\mathbf{x}, 0.01)$. We compute the adversarial robustness for $\ell_\infty(\epsilon = 0.01)$ to accommodate VisualPhishNet (Abdelnabi et al., 2020), and $\ell_2(\epsilon = 4)$ to provide comparisons for an alternative norm. In addition to PGD, we also investigate adversarial robustness towards the Carlini-Wagner (C&W) attack algorithm (Carlini & Wagner, 2017), which can be found in Appendix B.

Adversarial Training. Given that natural training of DML models is already considered an expensive procedure (Roth et al., 2020), solving the inner-maximization of

³This learning rate differs from the one stated by Roth et al. (2020) in their publication, 10^{-5} , but reflects the actual learning rate used throughout their experiments. See the field “lr” within experiment configuration: <https://bit.ly/3a4FyHP>.

the proposed robust formulations in Section 3.3 can make the procedure even more expensive and potentially infeasible for practical applications. As previously discussed, the inner-maximization is solvable using traditional first-order attack methods, e.g. FGSM, PGD, and C&W. This fact enables us to apply a training technique by Wong et al. (2020), that involves adversarial training using the cheaper R+FGSM (Tramèr et al., 2018) attack, in conjunction with early-stopping. This yields similar increases in robustness towards stronger and more expensive attacks, such as PGD, despite not being directed trained on these attacks. For this attack, we define $\alpha = \epsilon \cdot 0.25$ as we have empirically determined that it is effective and training DML models. Using the proposed attack algorithm for adversarial training (Section 3.5), we perturb the positive data points. This choice was to avoid affecting the relative distances to negative data points, which can induce instabilities during the training of DML models if they become too small (Wu et al., 2017).

Evaluation Metrics. To evaluate the performance of the trained models, we employ the following DML-specific evaluation metrics: Recall at One (R@1) and Mean Average Precision at R (mAP@R) (Musgrave et al., 2020). R@1 is effectively the accuracy of class inference using the class of the nearest neighboring anchor within the embedding space produced by the model. Given the test set $S = \{(\mathbf{x}_1, y_1), \dots, (\mathbf{x}_n, y_n)\}$, and the function $I_k(i)$ that outputs the indices of the k -nearest neighbors for a data point \mathbf{x}_i , such that

$$I_k(i) = \arg \min_{\substack{|K|=k \\ i \notin K}} \sum_{j \in K} d_\theta(\mathbf{x}_i, \mathbf{x}_j), \quad (18)$$

then R@1 given by:

$$\text{R@1} = \frac{1}{n} \sum_{\substack{i \in \{1, \dots, n\} \\ j \in I_1(i)}} 1_{y_i=y_j}. \quad (19)$$

mAP@R is metric for measuring a model’s ability to rank classes in the embedding space; we adopted this metric for the reasons covered by Musgrave et al. (2020). It is defined as

$$\text{mAP@R} = \frac{1}{n} \sum_{i=1}^n \frac{1}{R_i} \sum_{k=1}^{R_i} \frac{1}{k} \sum_{j \in I_k(i)} 1_{y_i=y_j}, \quad (20)$$

where $R_i = \sum_{j \in \{1, \dots, n\} \setminus \{i\}} 1_{y_i=y_j}$.

4.2. Experimental Results

Robustness of Natural Training (Q1) We establish a baseline of robustness against adversarial perturbations for naturally-trained DML models across the covered metric

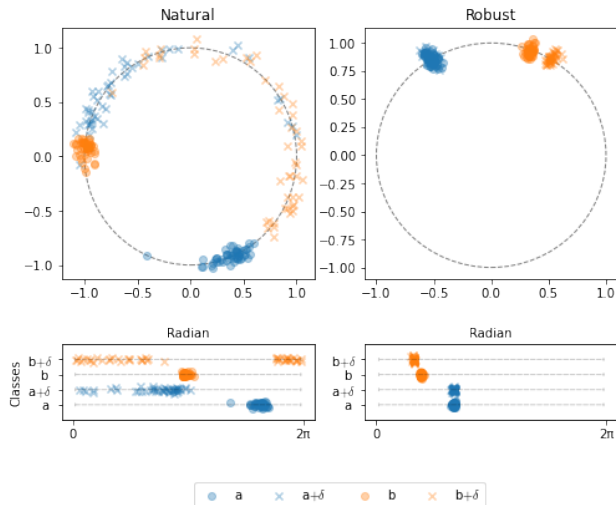


Figure 2. Embedding spaces of two trained models. (first row) Visualization of the embedding spaces of the two models (natural and robust). Effectively the embeddings are normalized to the unit circle, however, small distortions are added to improve visual clarity. Circles mark embeddings of benign data points, while crosses are data points with an adversarial perturbation (δ). (second row) Alternative visualization of the embedding space, showing the point relative to their radian on isolated spheres. It can be seen that embeddings of the robustly-trained model shifts much less, when faced with adversarial perturbed input, and are thus more robust.

losses, ℓ_p -norms, and datasets. Results can be seen in Table 1. Across any of the common real-world datasets (CUB200-2011, CARS196, SOP) it can be seen that both the model’s ability to infer the correct class from its nearest neighbor (R@1) and its ability to rank classes (mAP@R) drops by several orders of magnitude. Exemplifying this, the naturally-trained model using triplet loss on CUB200-2011 drops from 59.3% accuracy (on benign data) down to 4.0% (on adversarially-perturbed data) for $\ell_\infty(\epsilon = 0.01)$. Naturally-trained models on CARS196 and SOP yield comparable or worse adversarial robustness. Notably, naturally-trained models on the VisualPhish dataset achieves a higher baseline for adversarial robustness. We suspect this deviation, from the other common real-world datasets, is related to the underlying data distribution of the dataset.

We conclude that naturally-trained DML models are not inherently robust, contrary to what results of prior work might indicate (Abdelnabi et al., 2020). We suspect this difference might stem from the method of attack or the fact we use a stronger first-order attack.

Adversarial Training for Robustness (Q2) From Table 1, it can be seen that the proposed method for adver-

sarial training increases adversarial robustness (accuracy and ability to rank) across the chosen metric losses, norms, attacks and datasets. As an example, the robust R@1 on SOP increases from 0.7% (naturally-trained) to 56.3% for $\ell(\epsilon = 0.01)$. We also observe that the proposed method increases the adversarial robustness (in terms of R@1) on the VisualPhish dataset to 56.7%, and thus outperforms the prior work of VisualPhishNet (Abdelnabi et al., 2020), which achieves 42.8%. As shown in Appendix B, it can be seen that the gained robustness also applies to alternative attacks (C&W) for $\ell_2(\epsilon = 4)$. Performance of the trained robust models on benign input remains largely unaffected. Figure 1 shows an example of inference under different training objectives, and we provide a publicly available gallery of other examples⁴.

Effects on Embedding Space (Q3) Using the described synthetic dataset, we investigate the effect of adversarial training on the learned embedding space. The experiment involves training a DML model to map data points of the high-dimensional synthetic dataset, with the classes a and b , onto to a two-dimensional embedding space. We choose to have the embedding space be two-dimensional to allow visualizations of the learned embedding space. Each of the models, naturally-trained and robust, uses contrastive loss and is trained on approximately 15K data points. Adversarial perturbations are derived using the proposed attack formulation with PGD under $\ell_\infty(\epsilon = 0.01)$. Differences of the learned embedding spaces, and the influence of the adversarial perturbations, is shown in Figure 2. We observe that the robust model is capable of maintaining smaller inter-class distances between adversarially perturbed data points and benign data points.

5. Conclusion

Deep Metric Learning (DML) creates feature embedding spaces where similar input points are geometrically close to each other, while dissimilar points are far apart. However, the underlying DNNs are vulnerable to adversarial inputs, thus making the DML models themselves vulnerable. We demonstrate that naturally-trained DML models are vulnerable to strong attackers, similar to other types of deep learning models. To create robust DML models, we contribute a robust training objective that can account for the *dependence* of metric losses — the phenomenon that the loss at any point depends on the other items in the mini-batch and the sampling process that was used to derive the mini-batch. Our robust training formulation yields robust DML models that can withstand PGD attacks without severely degrading their performance on benign inputs.

⁴(anonymized gallery) <https://anonymous-koala-supporter.github.io/sample-gallery/>

References

- Abdelnabi, S., Krombholz, K., and Fritz, M. VisualPhish-Net: Zero-Day Phishing Website Detection by Visual Similarity. In *Proceedings of the 2020 ACM SIGSAC Conference on Computer and Communications Security, CCS 2020, November 9-13, 2020*. ACM, 2020.
- Ben-Tal, A., El Ghaoui, L., and Nemirovski, A. *Robust Optimization*. Princeton Series in Applied Mathematics. Princeton University Press, October 2009.
- Biggio, B., Corona, I., Maiorca, D., Nelson, B., Šrndić, N., Laskov, P., Giacinto, G., and Roli, F. Evasion attacks against machine learning at test time. *Lecture Notes in Computer Science*, pp. 387–402, 2013. ISSN 1611-3349. doi: 10.1007/978-3-642-40994-3_25. URL http://dx.doi.org/10.1007/978-3-642-40994-3_25.
- Boudiaf, M., Rony, J., Ziko, I. M., Granger, E., Pedersoli, M., Piantanida, P., and Ayed, I. B. A unifying mutual information view of metric learning: cross-entropy vs. pairwise losses. In *European Conference on Computer Vision*, pp. 548–564. Springer, 2020.
- Carlini, N. and Wagner, D. Towards evaluating the robustness of neural networks. In *2017 IEEE Symposium on Security and Privacy (SP)*, pp. 39–57, 2017.
- Chechik, G., Sharma, V., Shalit, U., and Bengio, S. Large scale online learning of image similarity through ranking. *J. Mach. Learn. Res.*, 11:1109–1135, March 2010. ISSN 1532-4435.
- Dan, C., Wei, Y., and Ravikumar, P. Sharp statistical guarantees for adversarially robust gaussian classification. *CoRR*, abs/2006.16384, 2020.
- Deng, J., Guo, J., Xue, N., and Zafeiriou, S. Arcface: Additive angular margin loss for deep face recognition. *2019 IEEE/CVF Conference on Computer Vision and Pattern Recognition (CVPR)*, Jun 2019. doi: 10.1109/cvpr.2019.00482. URL <http://dx.doi.org/10.1109/CVPR.2019.00482>.
- Duan, Y., Zheng, W., Lin, X., Lu, J., and Zhou, J. Deep Adversarial Metric Learning. In *2018 IEEE/CVF Conference on Computer Vision and Pattern Recognition*, pp. 2780–2789, 2018.
- Goldberger, J., Hinton, G. E., Roweis, S., and Salakhutdinov, R. R. Neighbourhood components analysis. *Advances in neural information processing systems*, 17: 513–520, 2004.
- Goodfellow, I., Pouget-Abadie, J., Mirza, M., Xu, B., Warde-Farley, D., Ozair, S., Courville, A., and Bengio, Y. Generative adversarial nets. In Ghahramani, Z., Welling, M., Cortes, C., Lawrence, N. D., and Weinberger, K. Q. (eds.), *Advances in Neural Information Processing Systems 27*, pp. 2672–2680. Curran Associates, Inc., 2014. URL <http://papers.nips.cc/paper/5423-generative-adversarial-nets.pdf>.
- Hadsell, R., Chopra, S., and LeCun, Y. Dimensionality reduction by learning an invariant mapping. In *Proceedings of the 2006 IEEE Computer Society Conference on Computer Vision and Pattern Recognition - Volume 2, CVPR '06*. IEEE Computer Society, 2006. doi: 10.1109/CVPR.2006.100. URL <https://doi.org/10.1109/CVPR.2006.100>.
- He, K., Zhang, X., Ren, S., and Sun, J. Deep Residual Learning for Image Recognition. *2016 IEEE Conference on Computer Vision and Pattern Recognition (CVPR)*, Jun 2016.
- Hein, M. and Andriushchenko, M. Formal guarantees on the robustness of a classifier against adversarial manipulation. In *Proceedings of the 31st International Conference on Neural Information Processing Systems*, pp. 2263–2273, 2017.
- Hermans, A., Beyer, L., and Leibe, B. In defense of the triplet loss for person re-identification. *ArXiv*, abs/1703.07737, 2017.
- Kingma, D. P. and Ba, J. Adam: A method for stochastic optimization. In *International Conference on Learning Representations (ICLR)*, 2015.
- Krause, J., Stark, M., Deng, J., and Fei-Fei, L. 3d object representations for fine-grained categorization. In *4th International IEEE Workshop on 3D Representation and Recognition (3dRR-13)*, Sydney, Australia, 2013.
- Li, P., Yi, J., Zhou, B., and Zhang, L. Improving the robustness of deep neural networks via adversarial training with triplet loss. In *Proceedings of the Twenty-Eighth International Joint Conference on Artificial Intelligence, IJCAI-19*, pp. 2909–2915. International Joint Conferences on Artificial Intelligence Organization, 7 2019. doi: 10.24963/ijcai.2019/403. URL <https://doi.org/10.24963/ijcai.2019/403>.
- Madry, A., Makelov, A., Schmidt, L., Tsipras, D., and Vladu, A. Towards deep learning models resistant to adversarial attacks. In *International Conference on Learning Representations*, 2018. URL <https://openreview.net/forum?id=rJzIBfZAb>.
- Mao, C., Zhong, Z., Yang, J., Vondrick, C., and Ray, B. Metric learning for adversarial robustness, 2019.

- Musgrave, K., Belongie, S., and Lim, S.-N. A metric learning reality check, 2020.
- Panum, T. K., Hageman, K. D., Hansen, R. R., and Pedersen, J. M. Towards Adversarial Phishing Detection, 2020.
- Roth, K., Brattoli, B., , and Ommer, B. Mic: Mining interclass characteristics for improved metric learning. *2019 IEEE/CVF International Conference on Computer Vision (ICCV)*, Oct 2019. doi: 10.1109/iccv.2019.00809. URL <http://dx.doi.org/10.1109/ICCV.2019.00809>.
- Roth, K., Milbich, T., Sinha, S., Gupta, P., Ommer, B., and Cohen, J. P. Revisiting Training Strategies and Generalization Performance in Deep Metric Learning, 2020.
- Schroff, F., Kalenichenko, D., and Philbin, J. Facenet: A unified embedding for face recognition and clustering. *2015 IEEE Conference on Computer Vision and Pattern Recognition (CVPR)*, Jun 2015.
- Simonyan, K. and Zisserman, A. Very deep convolutional networks for large-scale image recognition. In Bengio, Y. and LeCun, Y. (eds.), *3rd International Conference on Learning Representations, ICLR 2015*, 2015.
- Sohn, K. Improved deep metric learning with multi-class n-pair loss objective. In *Proceedings of the 30th International Conference on Neural Information Processing Systems*, pp. 1857–1865, 2016.
- Song, H. O., Xiang, Y., Jegelka, S., and Savarese, S. Deep metric learning via lifted structured feature embedding. In *IEEE Conference on Computer Vision and Pattern Recognition (CVPR)*, 2016.
- Szegedy, C., Zaremba, W., Sutskever, I., Bruna, J., Erhan, D., Goodfellow, I., and Fergus, R. Intriguing properties of neural networks. In *International Conference on Learning Representations*, 2014. URL <http://arxiv.org/abs/1312.6199>.
- Szegedy, C., Liu, W., Jia, Y., Sermanet, P., Reed, S., Anguelov, D., Erhan, D., Vanhoucke, V., and Rabinovich, A. Going Deeper with Convolutions. In *Computer Vision and Pattern Recognition (CVPR)*, 2015.
- Tramèr, F. and Boneh, D. Adversarial training and robustness for multiple perturbations. In *2019 Conference on Neural Information Processing Systems (NeurIPS)*, volume 32, 2019.
- Tramèr, F., Boneh, D., Kurakin, A., Goodfellow, I., Papernot, N., and McDaniel, P. Ensemble adversarial training: Attacks and defenses. In *6th International Conference on Learning Representations, ICLR 2018-Conference Track Proceedings*, 2018.
- Tsipras, D., Santurkar, S., Engstrom, L., Turner, A., and Madry, A. Robustness may be at odds with accuracy. In *In 7th International Conference on Learning Representations (ICLR)*, 2019.
- Vershynin, R. *High-Dimensional Probability: An Introduction with Applications in Data Science*. Cambridge University Press, 2018.
- Wang, X., Han, X., Huang, W., Dong, D., and Scott, M. R. Multi-similarity loss with general pair weighting for deep metric learning. *2019 IEEE/CVF Conference on Computer Vision and Pattern Recognition (CVPR)*, Jun 2019. doi: 10.1109/cvpr.2019.00516. URL <http://dx.doi.org/10.1109/CVPR.2019.00516>.
- Welinder, P., Branson, S., Mita, T., Wah, C., Schroff, F., Belongie, S., and Perona, P. Caltech-UCSD Birds 200. Technical Report CNS-TR-2010-001, California Institute of Technology, 2010.
- Wong, E., Rice, L., and Kolter, J. Z. Fast is better than free: Revisiting adversarial training. In *8th International Conference on Learning Representations, ICLR 2020, Addis Ababa, Ethiopia, April 26-30, 2020*, 2020. URL <https://openreview.net/forum?id=BJx040EFvH>.
- Wu, C.-Y., Manmatha, R., Smola, A. J., and Krahenbuhl, P. Sampling matters in deep embedding learning. *2017 IEEE International Conference on Computer Vision (ICCV)*, Oct 2017. doi: 10.1109/iccv.2017.309. URL <http://dx.doi.org/10.1109/ICCV.2017.309>.
- Xiao, K., Engstrom, L., Ilyas, A., and Madry, A. Noise or signal: The role of image backgrounds in object recognition, 2020.
- Xuan, H., Stylianou, A., and Pless, R. Improved embeddings with easy positive triplet mining. In *Proceedings of the IEEE/CVF Winter Conference on Applications of Computer Vision*, pp. 2474–2482, 2020.
- Yuan, Y., Yang, K., and Zhang, C. Hard-aware deeply cascaded embedding. In *Proceedings of the IEEE international conference on computer vision*, pp. 814–823, 2017.
- Zheng, W., Chen, Z., Lu, J., and Zhou, J. Hardness-aware deep metric learning. In *Proceedings of the IEEE/CVF Conference on Computer Vision and Pattern Recognition*, pp. 72–81, 2019.

A. Training Parameters (Expanded)

This section expands upon details and hyper-parameters used throughout the training of the respective DML models.

Batches & Sampling. Recall, that the training process uses a mini-batch size of 112 data points. Each mini-batch is sampled such that it contains exactly two samples per class (Roth et al., 2020). Following this, sets of tuples or triplets are derived (depended on loss) from the mini-batch using distance weighted sampling (Wu et al., 2017) for negatives, while positives are given by pair-based sampling. Distance weighted sampling enhances the stability of training using metric losses, that can suffer from becoming stuck at a local minima early on in the training procedure (Wu et al., 2017). The cardinality of the triplet-set is identical to the mini-batch size. The size of the tuple-set is double the size of the mini-batch, thus balancing out the number of data points being compared relative to the triplet-set. Furthermore, each data point within the tuple-set is used in a positive and negative pair.

Data Augmentation. We augment the dataset using the following operations for each input image: (1) random cropping to an image patch of size 60-100% of the original image area; (2) scaling; (3) normalization of pixel intensities. One difference is that our patch sizes differ from Roth et al. (2020) that employs patches of size 8-100% of original area. We change this parameter because recent work suggests that computer vision models can be biased by backgrounds and textures during during (Xiao et al., 2020). To combat this, we use cropping and scaling values based on Szegedy et al. (2015).

B. Alternative Attack (Carlini-Wagner)

The Carlini-Wagner (C&W) attack is an unbounded attack, and thus constrains perturbations to lie within the given ℓ_p (Carlini & Wagner, 2017). We employ a clipping technique similar to Tramèr & Boneh (2019), which projects the perturbation to the ℓ_p -ball at every step. Additionally, as inference is costly for DML models (nearest neighbor search across embedding space), the ability of providing early stopping mechanism has been disabled. Results are presented in Table 2. This is our best effort on providing strong hyper-parameters for the attack. It can be seen that the robustly trained model manages to remain higher robustness towards C&W attacks than the stronger PGD attack. The impact of the mentioned alterations, and the used hyper-parameters could yield the C&W attack to be non-optimal. Thereby, these results should be seen as an lower-bound representation of robustness towards the C&W, despite PGD generally being consider the state-of-

the-art (Wong et al., 2020).

C. Theoretical Analysis

C.1. Robustness and Lipschitzness of DML

In Section 1, we pointed out that the Lipschitzness of the DML model also plays an important role as in the traditional classifier situation. Here we have a formal analysis.

Let the sample space \mathcal{X} be $\bigcup_{y \in \mathcal{Y}} \mathcal{X}_y$, where $\mathcal{Y} = \{y_1, \dots, y_L\}$ is the space of labels and $\mathcal{X}_y \subseteq \mathcal{X}$ is the set of samples with label y . Suppose we have a deep embedding model f_θ with parameter θ trained using one of the loss functions described earlier. Let $A = \{(\mathbf{a}_1, c_1), \dots, (\mathbf{a}_m, c_m)\}$ be a reference dataset (e.g. a set of faces along with their label), which we call *anchors*. Suppose we have a sample \mathbf{z} and let $k(A, \mathbf{z})$ be the index that corresponds to $\arg \min_{j \in \{1, \dots, m\}} d_\theta(\mathbf{a}_j, \mathbf{z})$. We predict the label of \mathbf{z} as $lb(A, \mathbf{z}) = c_{k(A, \mathbf{z})}$. Recall that $d_\theta(\mathbf{x}, \mathbf{z})$ is the distance metric in the embedding space $\|f_\theta(\mathbf{x}) - f_\theta(\mathbf{z})\|_2$.

We will assume that our sample space \mathcal{X} is a metric space with metric μ . A point $\mathbf{z} \in \mathcal{X}$ is ϵ -robust w.r.t. A , μ and d_θ iff for $k(A, \mathbf{z}) = \arg \min_{1 \leq i \leq m} d_\theta(a_i, \mathbf{z})$, we have that for all $j \neq k(A, \mathbf{z})$ and $\mu(\mathbf{x}, \mathbf{z}) \leq \epsilon$, $d_\theta(a_j, \mathbf{x}) > d_\theta(a_{k_\mu(A, \mathbf{z})}, \mathbf{x})$. In other words, perturbing \mathbf{z} by ϵ in the sample space does not change the anchor it is close to in the embedding space.

A point $\mathbf{z} \in \mathcal{X}$ is δ -separated w.r.t. A and d_θ iff for $k(A, \mathbf{z}) = \arg \min_{1 \leq i \leq m} d_\theta(a_i, \mathbf{z})$ we have that for all $j \neq k(A, \mathbf{z})$, $d_\theta(a_j, \mathbf{z}) > d_\theta(a_{k_\mu(A, \mathbf{z})}, \mathbf{z}) + \delta$. In other words, $f_\theta(\mathbf{z})$ is at least δ closer to its anchor than other anchors in the embedding space. As a result, f_θ correctly classifies \mathbf{z} .

We assume that d_θ is L -Lipschitz, i.e., for all \mathbf{x} and \mathbf{z} in \mathcal{X} :

$$d_\theta(\mathbf{x}, \mathbf{z}) \leq L\mu(\mathbf{x}, \mathbf{z})$$

Lemma 1. If $L \leq \delta/(2\epsilon)$, and \mathbf{z} is δ -separated w.r.t. A and d_θ , then \mathbf{z} is ϵ -robust.

Proof. Let $i = k(A, \mathbf{x})$, $j \neq i$, and $\mu(\mathbf{x}, \mathbf{z}) \leq \epsilon$.

$$\begin{aligned} d_\theta(a_i, \mathbf{x}) &\leq d_\theta(\mathbf{x}, \mathbf{z}) + d_\theta(\mathbf{z}, a_i) \\ &\leq L\mu(\mathbf{x}, \mathbf{z}) + d_\theta(\mathbf{z}, a_i) \\ &< L\mu(\mathbf{x}, \mathbf{z}) + d_\theta(\mathbf{z}, a_j) - \delta \\ &\leq L\mu(\mathbf{x}, \mathbf{z}) + [d_\theta(\mathbf{z}, \mathbf{x}) + d_\theta(\mathbf{x}, a_j)] - \delta \\ &\leq L\mu(\mathbf{x}, \mathbf{z}) + L\mu(\mathbf{z}, \mathbf{x}) + d_\theta(\mathbf{x}, a_j) - \delta \end{aligned}$$

Because $L \leq \delta/(2\epsilon)$, $\mu(\mathbf{z}, \mathbf{x}) \leq \epsilon$, we have

$$d_\theta(a_j, \mathbf{x}) > d_\theta(a_i, \mathbf{x}) + (\delta - 2L\epsilon) \geq d_\theta(a_i, \mathbf{x}),$$

Table 2. Performance of robust DML models over four datasets for $\ell_2(\epsilon = 4)$ against the C&W attack algorithms. Results are an average of five random seeds. Recall that, R@1 reflects a model’s inference accuracy, while mAP@R reflects its ability to rank similar entities. Our robust training objective also provides robustness towards C&W attacks.

Model	Attack	CUB200-2011		CARS196		SOP		VisualPhish	
		R@1	mAP@R	R@1	mAP@R	R@1	mAP@R	R@1	mAP@R
$\ell_2(\epsilon = 4)$									
Contrastive (ℓ_2)	PGD	26.4 ± 0.3	11.1 ± 0.0	37.2 ± 0.2	9.7 ± 0.0	51.6 ± 0.0	29.2 ± 0.0	56.6 ± 0.4	54.0 ± 0.2
	C&W	40.6 ± 0.4	17.2 ± 0.1	58.7 ± 0.2	16.4 ± 0.0	63.2 ± 0.0	37.2 ± 0.0	67.8 ± 0.2	64.6 ± 0.1
Triplet (ℓ_2)	PGD	27.2 ± 0.2	11.3 ± 0.1	37.0 ± 0.4	9.3 ± 0.0	37.7 ± 0.1	20.3 ± 0.0	55.1 ± 0.1	50.9 ± 0.2
	C&W	42.0 ± 0.1	17.7 ± 0.1	59.6 ± 0.1	16.4 ± 0.0	54.5 ± 0.0	30.5 ± 0.0	68.7 ± 0.2	65.8 ± 0.2

so

$$d_\theta(a_i, \mathbf{x}) < d_\theta(a_j, \mathbf{x}).$$

□

C.2. DML with Gaussian Mixture Model

To further motivate the connection between robustness of an embedding and its Lipschitz constant, we consider a Gaussian mixture model. These models have been considered in the theoretical analysis of robustness in the classification setting (Dan et al., 2020; Tsipras et al., 2019). Our synthetic dataset experiment (Figure 2) illustrates this Gaussian mixture model setting. Let $\mathcal{N}(\mu, \Sigma)$ be the Gaussian distribution in \mathbb{R}^n with mean $\mu \in \mathbb{R}^n$ and Σ a $n \times n$ positive-definite matrix. We will consider Gaussian distributions of the form $\mathcal{N}(\mu, I_n)$ where I_n is the $n \times n$ identity matrix.

Let $\mathcal{X} \times \mathcal{Y}$ (where $\mathcal{Y} = \{-1, 1\}$) be generated from a distribution \mathcal{D} as follows: $y \in \mathcal{Y}$ is equally probable with probability $\frac{1}{2}$ and given y , generate \mathbf{x} according to $\mathcal{N}(y\mu, I_n)$.

We have the following concentration of measure result from Theorem 5.2.2 (Vershynin, 2018).

Theorem 1. (Gaussian concentration) Consider a random vector $\mathbf{x} \sim \mathcal{N}(0, I_n)$ and a Lipschitz function $f : \mathbb{R}^n \rightarrow \mathbb{R}$. Then

$$\|f(\mathbf{z}) - Ef(\mathbf{x})\|_{\psi_2} \leq C \|f\|_{Lip},$$

where $\|f\|_{Lip}$ is the Lipschitz constant of f , and $\|\cdot\|_{\psi_2}$ is the sub-Gaussian metric.

Consider a DML model $f_\theta : \mathbb{R}^n \rightarrow S^d$, and let d_θ be the associated distance metric. Let a_1 and a_{-1} be the anchors for labels 1 and -1 respectively. Consider the two functions defined as follows: $f_1(\mathbf{x}) = d_\theta(a_1, \mathbf{x})$ and $f_{-1}(\mathbf{x}) = d_\theta(a_{-1}, \mathbf{x})$ (the functions correspond to the distances from the two anchors).

$$\begin{aligned} \beta_1 &= E_{\mathbf{x} \sim \mathcal{N}(\mu, I_n)} f_1(\mathbf{x}) \\ \beta_{-1} &= E_{\mathbf{x} \sim \mathcal{N}(-\mu, I_n)} f_2(\mathbf{x}) \end{aligned}$$

We first show that f_1 is L -Lipschitz if f_θ is L -Lipschitz. Take $\mathbf{x}, \mathbf{z} \in \mathcal{X}$,

$$\begin{aligned} |f_1(\mathbf{x}) - f_1(\mathbf{z})| &= |d_\theta(a_1, \mathbf{x}) - d_\theta(a_1, \mathbf{z})| \\ &\leq d_\theta(\mathbf{x}, \mathbf{z}) \\ &\leq L\mu(\mathbf{x}, \mathbf{z}) \end{aligned}$$

As a result, $\|f_1\|_{Lip} = \|f_\theta\|_{Lip}$. Intuitively, if the Lipschitz constant of f_1 is lower, the points drawn from $\mathcal{N}(\mu, I_n)$ get closer to β_1 . In other words, as the Lipschitz constant of embedding gets smaller, the ‘‘point clouds’’ corresponding to the two Gaussian distributions in the mixture get farther apart, because they are concentrated more around their means.

Next we formalize this intuition. Let $E(\mathbf{x}, a_1, a_{-1})$ represent the event that \mathbf{x} is closer to a_{-1} than a_1 . We prove the following:

$$P_{\mathbf{x} \sim \mathcal{N}(\mu, I_n)}(1_{E(\mathbf{x}, a_1, a_{-1})}) \leq 2 \exp\left(-\frac{C' z^2}{\|f_1\|_{Lip}}\right) \quad (21)$$

In the equation given above, $C' > 0$ is a positive constant, and z is given by the following expression:

$$\frac{d_\theta(a_{-1}, a_1)}{2} - \beta_1$$

Notice that $P_{\mathbf{x} \sim \mathcal{N}(\mu, I_n)}(1_{E(\mathbf{x}, a_1, a_{-1})})$ represents the probability that a point drawn from $\mathcal{N}(\mu, I_n)$ is closer to a_{-1} than a_1 , and hence represents an ‘‘undesirable event’’. Also note that the upper bound goes down as the Lipschitz constant $\|f_1\|_{Lip}$ goes down, and thus confirming our intuition. Next we prove Equation 21.

Let X be a sub-Gaussian random variable, then the following equation is well-known:

$$P(|X| \geq t) \leq 2 \exp\left(-\frac{ct^2}{\|X\|_{\psi_2}^2}\right) \quad (22)$$

To prove the Equation 21, we use the following sequence of inequalities (let $q = P_{\mathbf{x} \sim \mathcal{N}(\mu, I_n)}(1_{E(\mathbf{x}, a_1, a_{-1})})$)

$$\begin{aligned}
 q &\leq P_{\mathbf{x} \sim \mathcal{N}(\mu, I_n)} \left(f_1(\mathbf{x}) \geq \frac{d_\theta(a_{-1}, a_1)}{2} \right) \\
 &\leq P_{\mathbf{x} \sim \mathcal{N}(\mu, I_n)} \left(|f_1(\mathbf{x}) - \beta_1| \geq \frac{d_\theta(a_{-1}, a_1)}{2} - \beta_1 \right) \\
 &\leq 2 \exp \left(-\frac{C' z^2}{\|f_1\|_{Lip}} \right)
 \end{aligned}$$

The first step follows from the following observation: if $f_1(\mathbf{x})$ is less than $\frac{d_\theta(a_{-1}, a_1)}{2}$ then \mathbf{x} is closer to a_1 than a_{-1} . The next two steps use Theorem 1 and Equation 22.